

# Measurement of secondary particle production induced by particle therapy ion beams impinging on a PMMA target

M. TOPPI<sup>1</sup>, G. BATTISTONI<sup>2</sup>, F. BELLINI<sup>3,4</sup>, F. COLLAMATI<sup>3,4</sup>,  
E. DE LUCIA<sup>1</sup>, M. DURANTE<sup>5</sup>, R. FACCINI<sup>3,4</sup>, P.M. FRALLICCIARDI<sup>6</sup>,  
M. MARAFINI<sup>3,4</sup>, I. MATTEI<sup>2</sup>, S. MORGANTI<sup>3</sup>, S. MURARO<sup>2</sup>,  
R. PARAMATTI<sup>3</sup>, V. PATERA<sup>3,6,7</sup>, D. PINCI<sup>3</sup>, L. PIERSANTI<sup>1,7</sup>,  
A. RUCINSKI<sup>3,7</sup>, A. RUSSOMANDO<sup>3,4,8</sup>, A. SARTI<sup>1,6,7</sup>, A. SCIUBBA<sup>3,6,7</sup>,  
M. SENZACQUA<sup>3,7</sup>, E. SOLFAROLI CAMILLOCCI<sup>8</sup>, G. TRAINI<sup>3,4</sup> and  
C. VOENA<sup>3,4</sup>

<sup>1</sup> INFN - Laboratori Nazionali di Frascati, Frascati (RM), Italy

<sup>2</sup> INFN, Sezione di Milano, Milano, Italy

<sup>3</sup> INFN, Sezione di Roma, Roma, Italy

<sup>4</sup> Dipartimento di Fisica, Sapienza Università di Roma, Roma, Italy

<sup>5</sup> GSI, Darmstadt, Germany

<sup>6</sup> Museo Storico della Fisica, Centro "E. Fermi", Roma, Italy

<sup>7</sup> Dipartimento di Scienze di Base e Applicate per Ingegneria, Sapienza  
Università di Roma, Roma, Italy

<sup>8</sup> Center for Life Nano Science@Sapienza, IIT, Roma, Italy

## Abstract

Particle therapy is a technique that uses accelerated charged ions for cancer treatment and combines a high irradiation precision with a high biological effectiveness in killing tumor cells [1]. Informations about the secondary particles emitted in the interaction of an ion beam with the patient during a treatment can be of great interest in order to monitor the dose deposition. For this purpose an experiment at the HIT (Heidelberg Ion-Beam Therapy Center) beam facility has been performed in order to measure fluxes and emission profiles of secondary particles produced in the interaction of therapeutic beams with a PMMA target. In this contribution some preliminary results about the emission profiles and the energy spectra of the detected secondaries will be presented.

# 1 Introduction

In particle therapy accelerated light ions ( $Z \leq 10$ ), especially p and  $^{12}\text{C}$ , are used for the treatment of tumors [1]. The greatest advantage of the particle therapy with respect to the conventional therapy with photons (radiotherapy) is a highly localized dose deposition, due to the typical profile of the dose released by a charged particle ending with the Bragg Peak, and hence a higher biological effectiveness in killing tumor cells. For such reasons this technique can be used for the treatment of highly radiation resistant tumors, sparing surrounding organs at risk (OAR) [2].

Due to the improved therapy spatial selectiveness, a novel monitoring technique, capable of providing a high precision “in-treatment” feedback on the dose release position, is required in order to act on the beam control and to prevent damages to OARs. Since the primary beam is fully stopped inside the patient body, it is necessary to exploit the secondary particles emitted in the nuclear interaction processes between the ion beam and the target nuclei, in order to reconstruct “online” the dose release [3–6]. Beyond p and  $^{12}\text{C}$  there is a growing interest in other ion beams like  $^4\text{He}$  and  $^{16}\text{O}$ : an improved characterization of the secondaries production for these beams is becoming crucial for their deployment in treatment centers. The precise knowledge of the secondary particles production, and in particular of their angular and energy distributions, is a key ingredient also for Treatment Planning Software (TPS) development, allowing to improve the MC description of the ion beams interaction with the patient body [9].

In this contribution we report about the data collected at the HIT beam facility (Heidelberg Ion-Beam Therapy Center), measuring the secondary particles produced in the interaction of  $^4\text{He}$ ,  $^{12}\text{C}$  and  $^{16}\text{O}$  beams, with therapeutic energies, against a beam stopping PMMA target. Three type of secondaries have been studied: charged fragments (from both projectile and target fragmentation), PET  $\gamma$  (from  $\beta^+$  emitters fragments) and prompt  $\gamma$  (from nuclear de-excitation), aiming to correlate the emission point with the dose release and to compute the production fluxes for each type of secondaries. In this contribution we present a brief description of the HIT experiment apparatus and the preliminary results about secondaries emission profiles and energy spectra.

## 2 The HIT experimental setup

The HIT experimental apparatus (Fig. 1, left) is composed of several subdetectors, each optimized for the detection of one or more type of secondaries

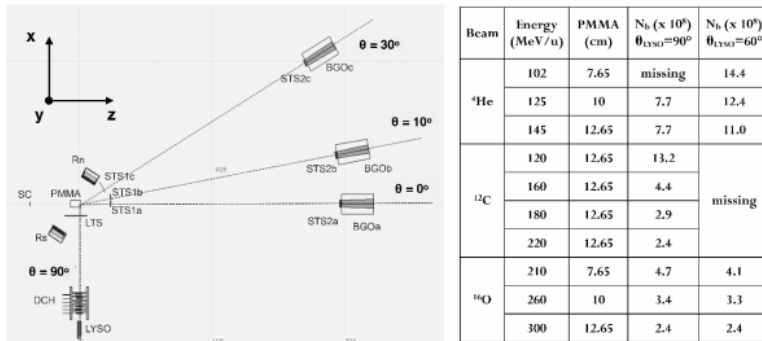


Figure 1: Left: HIT experimental setup (the scale along the three axis is in cm). Right: Table summarizing the different set up configurations, for each ion beam and for each beam energy. The number of primaries  $N_b$ , provided by the start counter detector (SC), is different for the two LYSO position ( $\theta_{\text{LYSO}} = 60^\circ, 90^\circ$ )

produced by the interaction of the ion beam with the PMMA target. For each ion beam different beam energies and geometrical configurations have been studied, as summarized in the table of Fig. 1 (right). The PMMA thickness has been changed, depending on the beam and on its energy, in order to keep the Bragg Peak always inside the target. Before interacting with the target the ion beam goes through the start counter (SC), a thin scintillator that provides the number of primary ions impinging on the PMMA target and that provides the triggers of the experiment in combination with other subdetectors.

The forward emitted charged fragments are detected by a system of three BGO crystals (truncated pyramids 24 cm thick and with square bases  $4.7 \times 4.7 \text{ cm}^2$  and  $6.0 \times 6.0 \text{ cm}^2$  respectively, read by EMI 98117B PMTs) and three pairs of thin plastic scintillators (STS1 -  $0.2 \times 4.0 \times 4.0 \text{ cm}^3$  and STS2  $1.0 \times 4.7 \times 4.7 \text{ cm}^3$ , read by H10580 PMTs) providing energy and ToF measurements. Each BGO and STS pair combination is an independent coaxial system positioned at different angular position ( $\theta \sim 0^\circ, 10^\circ, 30^\circ$ , with  $\theta$  emission angle respect to the beam direction  $z$ , as shown in Fig 1).

The charged fragments emitted at large angle, while having a reduced yield, can still be of interest for dose monitoring purpose because of their improved spatial resolution  $\sigma_z$  on the fragment emission point ( $\sigma_z \sim 1/\sin\theta$ , see [6]). The study of such large angle events is performed using a coaxial system composed of a thin plastic scintillator (LTS -  $0.2 \times 5.0 \times 17.0 \text{ cm}^3$ , read by a H10580 PMT), a drift chamber (DCH) and a LYSO crystals detector, already described in [6]. Data were acquired with this system placed at

$\theta \sim 60^\circ$  and  $90^\circ$  in order to measure the energy, the ToF and the emission angle  $\theta$  of the charged fragments. The same LYSO scintillator has also been used to measure the prompt  $\gamma$  energy spectra and the integrated production fluxes. Since no collimator was used during the data acquisition, the profile of the emission position of the prompt  $\gamma$  could not be measured.

In order to study the  $\beta^+$  emission, gaining access both to the position and to the flux, a device able to measure the energy and the ToF of the two back-to-back 511 keV  $\gamma$  in time coincidence was set up. Two pairs of PET heads, shown as Rn and Rs in Fig. 1, composed of a matrix of  $23 \times 23$  LYSO crystals each have been used.

A MC simulation of the full setup has been developed with FLUKA [7,8] for efficiencies and angular acceptances studies.

### 3 Preliminary results

Fig. 2 (left) shows the measured energy versus the ToF distribution for detected fragments ( $\theta = 10^\circ$ ) originating from the interactions of an  $^4\text{He}$  beam of 125 MeV/u energy with the PMMA. The three bands, that are clearly visible, are related to the hydrogen ions ( $^1\text{H}$ ,  $^2\text{H}$  and  $^3\text{H}$ ). The heavier fragments are not visible due to their smaller production cross section and their lower range. A similar behavior is observed for all the exploited ion beams.

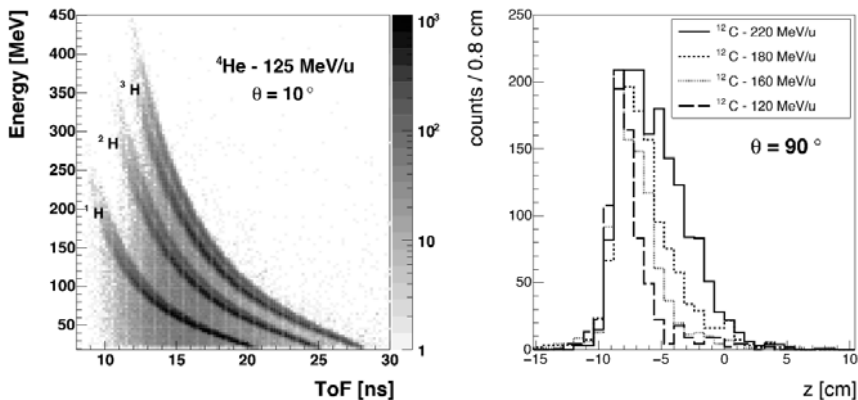


Figure 2: Left: Energy measured by the BGO vs the ToF measured by the STS of the setup at  $10^\circ$  for the charged fragments emitted in the case of the 125 MeV/u  $^4\text{He}$  beam. The bands corresponding at the  $^1\text{H}$ ,  $^2\text{H}$  and  $^3\text{H}$  fragments are clearly visible. Right: Emission profile of the charged fragments in the case of the  $^{12}\text{C}$  beam at different energies with LYSO detector at  $\theta = 90^\circ$ .

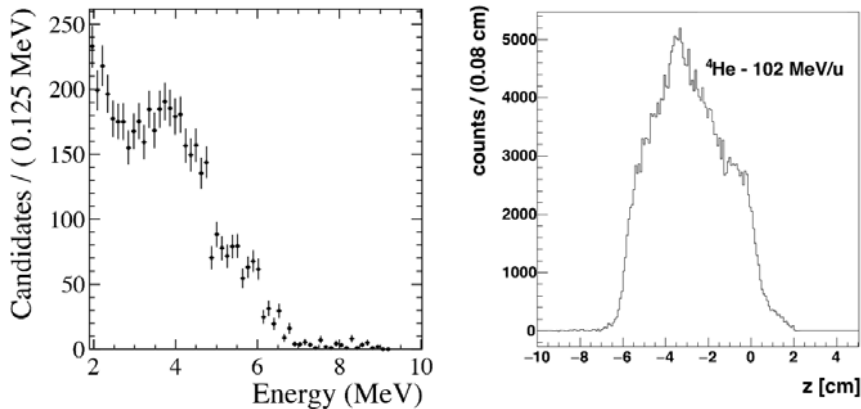


Figure 3: Left: prompt  $\gamma$  energy spectra in the case of the  $^{12}\text{C}$  beam. Right:  $\beta^+$  emission profile in the case of the  $^4\text{He}$  beam at 102 MeV/u.

The fragments yield at large angles is lower than the yield at small angle as expected from fragmentation cross sections measurements [10]. However a non negligible production of hydrogen ions at large angles is observed for all beam types. The large angle hydrogen ions emission shape can be correlated to the beam entrance window and the Bragg Peak position exploiting the LYSO detector, as already measured with  $^{12}\text{C}$  and discussed in [6]. Fig. 2 (right) shows the hydrogen ions reconstructed emission positions, along the  $z$  axis, measured at  $\theta = 90^\circ$ , for carbon beam of different energies.

The prompt  $\gamma$  produced by the nuclear de-excitation of ions and target nuclei along the beam path have been studied with the LYSO detector (measuring Energy and ToF), the SC detector (providing the trigger) and the LTS (used to veto the charged fragments). The energy spectra of the emitted  $\gamma$  have been measured, for all the different beam types and energies, using the LYSO detector to identify the prompt  $\gamma$  using the Energy vs ToF informations as described in [11]. In Fig. 3 (left) the measured energy spectra of the prompt  $\gamma$  emitted in the interaction of the  $^{12}\text{C}$  beam with the PMMA target in the case of the LYSO detector at  $\theta = 90^\circ$  is shown. Similar spectra have been obtained for all the beams and angular configurations ( $\theta = 60^\circ, 90^\circ$ ). These raw energy spectra have not yet been corrected for efficiencies or resolution effects in order to obtain the production energy spectra.

The PET heads have been used to study the  $^4\text{He}$  beam only. Due to the huge background coming from prompt  $\gamma$  and neutrons during the beam spill, the PET  $\gamma$  events have been selected in the time window with the beam off between two consequent spills (offspill) requiring the double time

coincidence of the Rn and Rs heads. In Fig. 3 (right) the  $\beta^+$  emitters profile has been reconstructed for the  $^4\text{He}$  beam at 102 MeV/u. The raw emission profile has yet to be corrected for the detector efficiencies and for the angular acceptance.

## 4 Conclusions

In this contribution the preliminary results for the secondaries emission spectra produced in the interaction of different ion beams ( $^4\text{He}$ ,  $^{12}\text{C}$  and  $^{16}\text{O}$ ) with a thick PMMA target have been presented.

## References

- [1] M. Durante and J. S. Loeffler, *Nat. Rev. Clin. Oncol.*, **7**, 37–43, (2010).
- [2] D. Schardt *et al.*, *Rev.Mod.Phys*, **82**, No. 1, 383–425, (2010).
- [3] E. Testa *et al.*, *Nucl. Instrum. Meth. B*, **267**, 993, (2009).
- [4] K. Parodi *et al.*, *Phys. Med. Biol.*, **47**, 21, (2002)
- [5] C. Agodi *et al.*, *Phys. Med. Biol.*, **57**, 5667, (2012)
- [6] L. Piersanti *et al.*, *Phys. Med. Biol.*, **59**, 1857–1872, (2014).
- [7] A. Ferrari *et al.*, CERN 2005-10, INFN/TC\_05/11, (2005).
- [8] T.T. Böhlen *et al.*, *Nuclear Data Sheets*, **120** (2014) pp. 211–214.
- [9] T.T. Böhlen *et al.*, *Phys. Med. Biol.*, **55**, 5833–47, (2010).
- [10] J. Dudouet *et al.*, *Physical Review C*, **88**, 024606, (2013).
- [11] C. Agodi *et al.*, *Journal of Instrumentation*, vol. **7**, P03001, (2012).